Pamukkale Üniversitesi Mühendislik Bilimleri Dergisi
Pamukkale University Journal of Engineering Sciences

# Improving photoreactor design with ansys fluent flow simulation

## Fotoreaktör tasarımının ansys fluent akış simülasyonuyla iyileştirilmesi

*Ali Canberk ÇOŞKUN[1], Dilek DURANOĞLU[1*]*

[1]Department of Chemical Engineering, Yıldız Technical University, Istanbul, Turkey.
alicanberkcoskun@gmail.com, dduran@yildiz.edu.tr

Received/Geliş Tarihi: 27.07.2023 Revision/Düzeltme Tarihi: 09.02.2024 doi: 10.5505/pajes.2024.27448
Accepted/Kabul Tarihi: 23.02.2024 Research Article/Araştırma Makalesi

**Abstract**

*Ansys Fluent can be used in chemical engineering to draw velocity profiles, temperature profiles inside pipes and columns and determine pressure losses, making 2D and 3D simulations of mass separation processes using user defined functions. Computational fluid dynamics (CFD) software can be applied for the analysis of photoreactors, which initiate and sustain chemical reactions through the application of light energy. Photoreactors can be used in a variety of industries and their performance can significantly impact the efficiency of the chemical processes they support. In this study, Ansys Fluent flow simulation was applied in order to improve the design of proposed photoreactor. Firstly, base photoreactor models were simulated via Ansys Fluent CFD software. Accordingly, these base models were further developed in order to obtain high fluid velocity and homogenous flow by adding baffles and nozzles. The effects of baffle height and spacing on the total velocity and flow homogeneity were also investigated. All models were analysed with the total fluid velocity on selected points and standard deviation between the velocity data. Optimal photoreactor design with the highest fluid velocity and homogenous flow distribution was developed.*

**Keywords:** Ansys Fluent, flow simulation, photoreactor design

**Öz**

*Ansys Fluent, kimya mühendisliğinde boru ve kolonların içindeki hız profillerini, sıcaklık profillerini çizmek ve basınç kayıplarını belirlemek, kullanıcı tanımlı fonksiyonları kullanarak kütle ayırma işlemlerinin 2 ve 3 boyutlu simülasyonlarını yapmak için kullanılabilir. Işık enerjisinin uygulanması yoluyla kimyasal reaksiyonları başlatan ve sürdüren fotoreaktörlerin analizinde de hesaplamalı akışkanlar dinamiği (CFD) yazılımı kullanılabilir. Çeşitli endüstrilerde kullanılan fotoreaktörlerin performansı, destekledikleri kimyasal süreçlerin verimliliğini önemli ölçüde etkileyebilir. Bu çalışmada, önerilen fotoreaktörün tasarımını iyileştirmek için Ansys Fluent akış simülasyonu uygulanmıştır. İlk olarak, üç temek fotoreaktör modeli Ansys Fluent CFD yazılımı ile simüle edilmiştir. Buna göre, yüksek akışkan hızı ve homojen akış elde etmek için, kanatçık ve nozullar eklenerek bu temel modeller geliştirilmiştir. Kanatçık yüksekliği ve aralığının toplam hız ve akış homojenliği üzerindeki etkileri de incelenmiştir. Tüm modeller, seçilen noktalardaki toplam akışkan hızı ve hız verileri arasındaki standart sapma ile analiz edilmiştir. Sonuç olarak, maksimum akışkan hızına ve homojen akış dağılımına sahip optimum fotoreaktör tasarımı geliştirilmiştir.*

**Anahtar kelimeler:** Ansys Fluent, akış simülasyonu, fotoreaktör tasarımı



## 1 Introduction

Computational Fluid Dynamics (CFD) is a powerful tool used in various fields, including cardiovascular medicine, fluid flow in porous media, coastal and offshore applications, acoustic wave propagation, fluid-structure interaction, and more. CFD models are developed to simulate and analyse the fluid flow and related phenomena, providing insights into complex systems that are difficult to study experimentally. These methods provide valuable insights into complex fluid flow phenomena and help improve diagnostic assessment, device design, and understanding of physical processes.

In cardiovascular medicine, CFD-based techniques are being increasingly applied to build computer models of the cardiovascular system in health and disease [1]. These models help to enhance diagnostic assessment, device design, and clinical trials. For example, Sacks & Yoganathan (2008) developed a sophisticated three-dimensional CFD model to study heart valve function. Their model, based on the curvilinear immersed boundary method, provided numerical simulations that described differences in shear stress patterns on the ventricular and aortic surfaces, which agreed with experimental observations [2]. In the study of Erdem et al. (2017), Finite Element Analysis were taken into consideration to simulate and model bone drilling, cutting and screwing processes [3]. In another article, the fatigue behaviours of different materials for Schanz screws in a femoral fracture model using finite element analysis were investigated [4].

In the field of fluid flow in porous media, CFD models are used to simulate multiphase fluid flow and reactive transport. Meakin & Tartakovsky (2009) discussed the application of multiscale methods, such as adaptive mesh refinement, for the large-scale continuum CFD simulations [5]. These methods improve the accuracy of multiphase fluid dynamics simulation. Additionally, particle-scale simulations using the discrete element method have been applied to study flow and heat transfer behaviours in fluidized bed [6].

CFD simulations are also valuable in coastal and offshore applications. Schmitt et al. (2019) present an implementation of an impulse source wave maker for CFD simulations, which allows for the generation of desired wave series in deep or shallow water [7]. This method, based on the open-source CFD software, OpenFOAM, accurately calibrates the phase and amplitude of wave packets. In the field of acoustic wave propagation, CFD models are used to simulate and analyse the behaviour of sound waves. Córdova et al. (2016) presented two fourth-order compact finite difference (CFD) discretization of

*Corresponding author/Yazışılan Yazar

the acoustic wave equation [8]. These discretization, implemented on rectangular grids, provide accurate results and demonstrate convergence as the grid is refined.

CFD methods are also applied to study fluid-structure interaction problems. Wang et al. (2011) discussed the challenges and solutions in treating wall boundary conditions and fluid-structure transmission conditions in embedded boundary methods for CFD [9]. They presented numerical methods for treating fluid pressure and velocity conditions on static and dynamic embedded interfaces, as well as approached for computing flow-induced loads on rigid and flexible structures. In another study [10], the lithium fluid was successfully analysed in a three-dimensional circular channel under exposing to external magnetic field induction by using Ansys Fluent. Moreover, Ansys Workbench was applied in order to simulate the negative effects of classical face masks and the use of silicone pads to prevent these effects [11].

Although CFD methods can be applied in the modelling and simulation of photoreactors, there are limited number of studies. Kovačič et al. (2020) discussed the use of CFD in the modelling of fluidized bed photoreactors for photocatalytic CO2 reduction [12]. They highlighted the importance of considering mass and heat transfer in the macro scale and presented a complete multiscale simulation using integrated particle, fluid, and photo behaviour models. In another study, inlet velocity effects on mass transfer was simulated via CFD simulation (COMSOL) for twin bubbling photocatalytic reactor [13]. It was showed that the bubbling twin reactor has better performance compared to traditional twin reactor in mass transfer, as well as production.

Photoreactors, where the light is used to drive chemical reactions, are used in photoredox chemistry or photocatalysis studies. Despite the increasing interest of photochemistry in recent years, photocatalysis is still seldom used in industry due to the limited number of study on photoreactor design. Photoreactor design is critical to perform accurate and reproducible photoredox and photocatalytic processes. Geometry of the photoreactors depends not only the irradiation source but also flow distribution, mass transfer, fluid flow regime, reaction kinetics etc. [14]. A proper description of the mass transport is crucial to determine limitations and obtain the conversions of reactants and formation of products in photoreactors [15]. The fluid flow and temperature distributions, and concentration profiles within the reactor can be investigated via CFD simulations easily. Hence, different reactor geometries without the need of physical prototypes can be designed. By this way, the researchers and industrial users save the time and economy.

In this study, lab-scale continuous type photoreactors were designed for the purpose of photocatalysis experiments. Ansys Fluent flow simulation was applied to improve the flow regime of the proposed photoreactors. For this purpose, first, proposed base photoreactor models, which have different inlet positions, were simulated via Ansys Fluent CFD software. Accordingly, these base models were further developed in order to obtain high fluid velocity and homogenous flow by adding baffles and nozzles. The effects of inlet position as well as the baffle height and spacing on the total velocity and flow homogeneity in a continuous type photoreactor were investigated for the first time in the literature.

# 2 Materials and Methods

## 2.1 Photoreactor models

Three base photoreactor models with different inlet positions were constructed as seen in Figure 1. These models were abbreviated as F10, F20 and F30 (Figure 1). The cylindrical photoreactor has a quartz holder inside of it. This quartz cylindrical holder contains the light source. The inlet/outlet flowrate is 50mL/min, which corresponds to 0.0423 m/s in terms of velocity for 5mm inlet diameter. All developed photoreactors volume kept around 500mL.

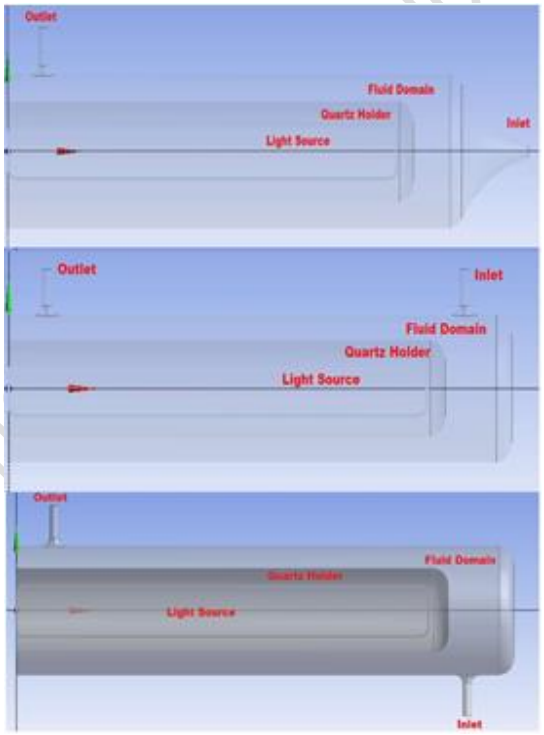


Figure 1. Base photoreactor models

Proposed base models were 3D drawn first, then, all models were simulated via Ansys Fluent CFD software. With the purpose of developing optimal photoreactor design, these base models were further developed in order to obtain high fluid velocity and homogenous flow inside the reactor. Firstly, baffles were added inside the photoreactor to increase the flow velocity. After that, nozzles were also added with baffles to increase the velocity and homogeneity. Total of 9 designs were investigated. The properties of these designs are shown in Table 1. Inlet/outlet diameter, quartz holder length/diameter and reactor volume given in the Table 1 were kept constant for all developed models.

Table 1. Properties of developed photoreactor models.

| | Baffle | | | Nozzle | |
|---|---|---|---|---|---|
| | Spacing (mm) | Height (mm) | Thickness (mm) | Diameter (mm) | No |
| F10 | n.a | n.a | n.a. | n.a. | n.a. |
| F11 | 11 | 5.6 | 4 | n.a. | n.a. |
| F12 | 11 | 2.5 | 4 | n.a. | n.a. |
| F13 | 22 | 2.5 | 4 | n.a. | n.a. |
| F14 | 11 | 5.6 | 4 | 2.5 | 6 |
| F20 | n.a. | n.a. | n.a. | n.a. | n.a. |
| F21 | 11 | 5.6 | 4 | n.a. | n.a. |
| F22 | 11 | 5.6 | 4 | 2.5 | 6 |

photoreactor diameter: 61.2 mm; inlet and outlet diameter: 5 mm; quartz holder length: 230mm; quartz holder diameter: 40 mm

### 2.2 ANSYS Fluent

The proposed photoreactor models were investigated and improved with the CFD simulation using (ANSYS 2021, academic version) in order to obtain optimum flow profile. It was aimed to obtain homogeneous flow distribution with high velocity. ANSYS Fluid Flow (fluent) analysis solver was used to perform the CFD simulations. It is based on the solution of conservation equations of the transferred fluid, using Element-Based Finite Volume Method. In this research, the conservation of total mass (continuity) and momentum (Navier-Stokes) equations given Eq. 1 and Eq. 2 were solved for incompressible, steady-state and turbulent inlet flow conditions.

$$\nabla \cdot \mathrm{U} = 0 \quad (1)$$

$$\rho\,(U \cdot \nabla U) = -\nabla P + \mu \nabla^2 U + \rho \cdot g \quad (2)$$

In Eq.1 and Eq.2, ρ is the density of the fluid, μ is the dynamic viscosity, U is the velocity vector, P is the pressure, g is the gravity. Average mesh skewness was 0.233 and the highest one was 0.755. Time frame steady type pressure based simple method was applied in fluent solver. The inlet boundary condition was selected as fluid inlet velocity and atmospheric pressure was set for the outlet. Water at constant temperature of 300K (density: 998.2 kg/m$^3$ and viscosity: 0.001003 kg/m.s) was examined as fluid flowing inside the photoreactor. The residual for error tolerance was 0.000001 for velocity and continuity.

## 3 Results and discussion

### 3.1 Ansys Flow Simulations of Base Models

After simulating via Ansys Fluent, obtained fluid flow velocity profile of three base models are given in Figure 2. In order to compare different models, 9 points were selected, and their velocities were determined and visualized in Figure 2. These points were named with the letters A,B,C,D,E,F,G,H and I. The purpose of the selection of these points are to see the velocity change from theinlet part of the photoreactor to outlet part. A,C and E are on the same horizontal line; B, D and F points are symmetrical points of these points to y-axis. G and H points are closer to thewall, and are also symmetrical to y-axis. Point I was selected with the purpose of seeing the velocity in the dead-zone of the photoreactor.

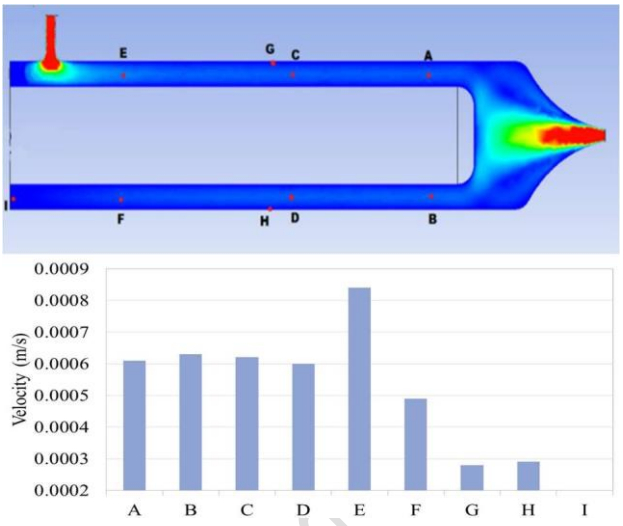


a) F10 (total velocity: 4.37x10$^{-3}$ m/s and standard deviation: 2.5x10$^{-4}$)

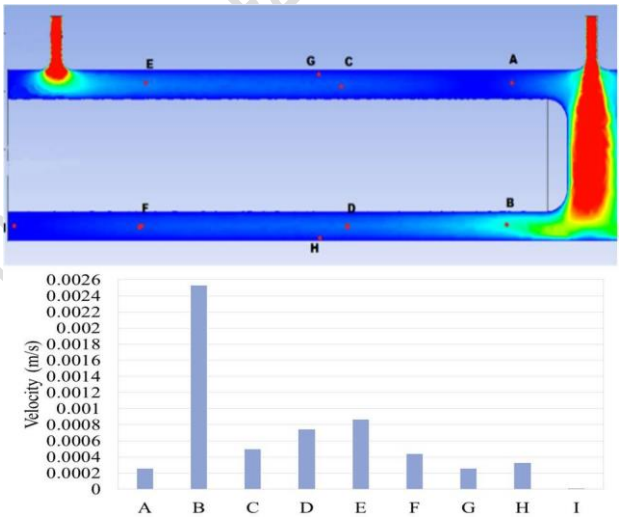


b) F20 (total velocity: 5.94x10$^{-3}$ m/s and standard deviation: 7.47x10$^{-4}$ )

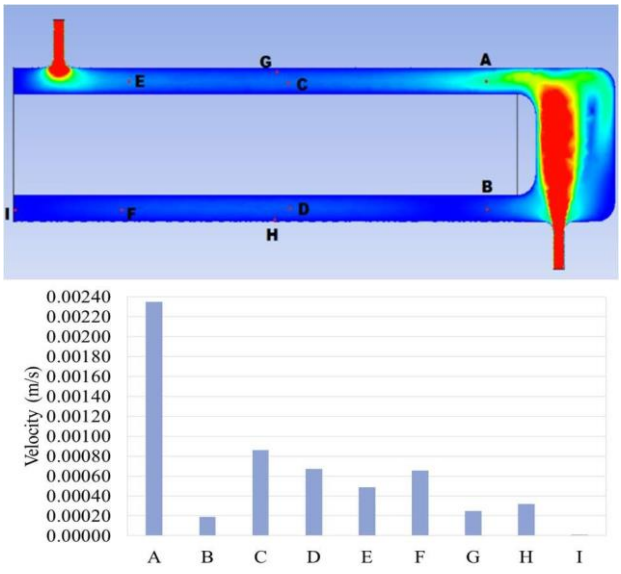


c) F30 (total velocity: 5.79x10-3 m/s and standard deviation:6.94x10$^{-4}$)

Figure 2. Flow simulation and fluid velocity variations of basephotreactor models.

The base model F10 has a side inlet which enables a better fluid distribution inside the photoreactor. The velocity, on the other hand, was not as high as wanted, but this geometry showed great potential for future improvements. Total fluid velocities at given points is $4.37x10^{-3}$ m/s and standard deviation is $2.5x10^{-4}$ for F10. As can be seen from the Figure 2a, A,B,C and D points have very similar velocities. This shows a great velocity distribution in those points. The main difference starts at the point E, which is close to the outlet of the photoreactor. E has a higher velocity than other points. F, the symmetrical point of E point to y-axis, has a much slower velocity. The main reason for this phenomena is, because the flow tends to head towards the outlet, which results in this velocity difference. G and H points have slower flows compared to C and D points. This is expected because when flow gets closer to the walls, its effected by friction, which decreases the velocity. On the point I, the flow is almost non-existent.

The base model F20 has an inlet from the top of the photoreactor. This comes with a velocity boost from gravity, but greatly disturbs the homogenous distribution of flow. Still, the higher velocity looks promising for the future improvements. Total fluid velocities at the given points is $5.94x10^{-3}$ m/s and standard deviation is $7.47x10^{-4}$ for F20. As can be seen from the Figure 2b that the flow distribution is very uneven. The point B has a velocity of almost 10 times of point A. Distribution improves in the points C, D, E and F, but still the velocity differences are significant. Even the homogeneity of the flow is very bad in this model, total high velocity looks promising. It was concluded that this model could be improved to make the flow more homogenous without losing the total high velocity.

The base model F30 has an inlet from the bottom of the photoreactor. This model resembles F20 model, but in this model, gravity does not help, the exact opposite, it becomes an obstacle for this mode. This is because flow goes from bottom to top but gravity pulls the fluid to the opposite direction, resulting in loss of acceleration. On the other hand, like F20, flow distribution is not homogenous. Total fluid flow velocities at given points is $5.79x10^{-3}$ m/s and standard deviation is $6.94x10^{-4}$ for F30. As can be seen from the figure 2c, similar to F20, there is a great difference in the distribution of the flow.

As a conclusion, among the base models, F10 has the most homogenous flow inside the photoreactor with relatively lower total fluid velocity. F20 and F30 also contain potential because of the higher total velocity. Due to the fact that both F20 and F30 showed the similar results, F20 model was chosen for the further improvements on fluid flow homogeneity.

### 3.2 Development of Base Models via Ansys Flow Simulation

#### 2.2.1 Ansys Flow Simulation of developed F10 models

In order to increase the homogeneity and total velocity in the flow of F10, the baffles were added to the F10 base model, hence, F11 were obtained (Figure 3b). Baffles in F11 have 4mm of thickness, 5.6mm of height and 11mm of spacing between each other. In order to compensate the volume loss caused by the baffles, reactor total length was increased 15mm.

Total fluid velocity at the given points is $8.63x10^{-3}$ m/s and standard deviation is $6.87x10^{-4}$ for F11. As can be seen from Figure 3b, baffles greatly improved the velocity and homogeneity in the points A,B,C,D,E and F. On the other hand, they caused dead-zones in the points of G and H. On average, total velocity and standard deviation increased. Then, different baffle spacing and baffle heights were applied to see the difference between more spaced and shortened baffles (F12, F13).

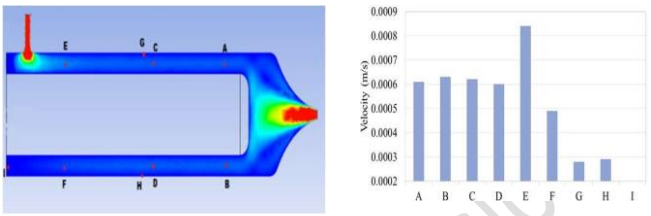


a)F10 (total velocity: $4.37x10^{-3}$ m/s and standard deviation: $2.5x10^{-4}$)

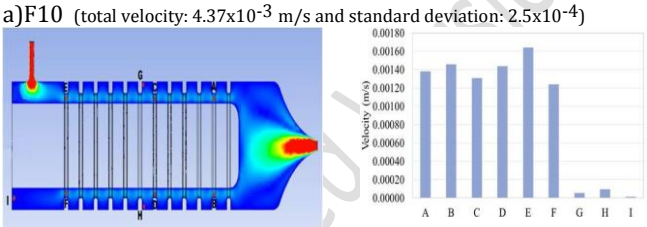


b)F11 (total fluid velocity: $8.63x10^{-3}$ m/s and standard deviation:$6.87x10^{-4}$)

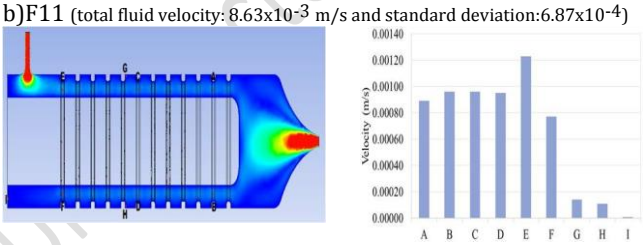


c)F12 (total fluid velocity: $6.02x10^{-3}$ m/s and standard deviation is $4.54x10^{-4}$)

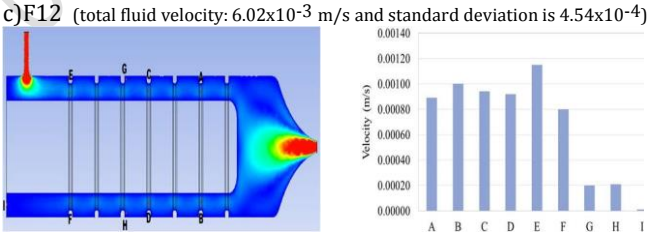


d)F13 (total fluid velocity: $6.12x10^{-3}$ m/s and standard deviation: 4.19x10-4)

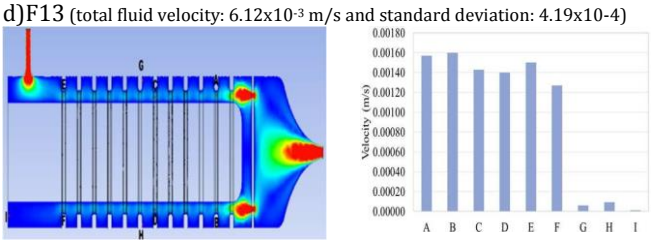


e)F14 (total fluid velocity: $8.94x10^{-3}$ m/s and standard deviation: $7.10x10^{-4}$)

Figure 3. Flow simulation and fluid velocity variations of developed F10 models.

F12 has the same baffle thickness and spacing as F11, but the baffle heights were reduced to 2.5mm. Total fluid velocity at given points is $6.02x10^{-3}$ m/s and standard deviation is $4.54x10^{-4}$ for F12. As can be seen from Figure 3c, velocities on every point except G and H have dropped. Reducing baffle heights from 5.6mm to 2.5mm greatly improved the standard deviation of the flow while costing total velocity to drop.

In the model F13, baffle spacing was doubled to 22mm from 11mm in order to decrease the dead-zones created due to the baffles. Total fluid velocity at given points is $6.12x10^{-3}$ m/s and standard deviation is $4.19x10^{-4}$ for F13. Increasing baffle spacing did not much increase the total velocity compared to the previous model (F12). Moreover, there is a velocity loss

between baffles.When the baffle spacing is lower, there are less space for fluid to travel without encountering a baffle, so frequency of fluid to encounter a baffle is higher. That means, on the un-recorded points, which are between the baffles, there is a velocity loss which is not included in the data.

The model F14 was developed using F11 as basis. 6 nozzles with 2.5mm diameter were added. Both total velocity and homogeneity was aimed to increase with nozzles. Total fluid velocity at given points is $8.94x10^{-3}$ m/s and standarddeviation is $7.10x10^{-4}$ for F14. As can be seen from the Figure 3d, there is a great velocity distribution on the points A,B,C,D,E and F, however, points G and H have very low velocity values. Nozzles greatly improved the flow homogeneity on points between A and F. Overall, this model offers significantly higher total velocity while having dead-zones between baffles.

### 2.2.2 Ansys Flow Simulation of developed F20 models

As can be seen in Figure 4, the base model F20 was improved with baffles (F21). The nozzles were also added, in order to eliminate the flow heterogeneity between the top and the bottom of the photoreactor (F22).

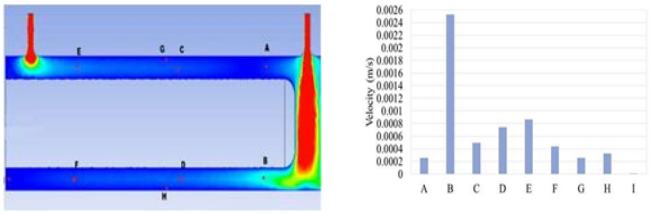


a)F20 (total fluid velocity:$5.94x10^{-3}$m/s; standard deviatio:$7.47x10^{-4}$)

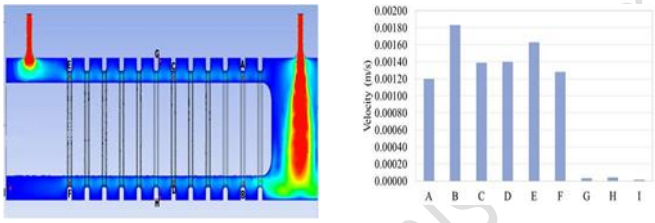


b)F21 (total fluid velocity:$8.82x10^{-3}$m/s; standard deviation:$7.36x10^{-4}$)

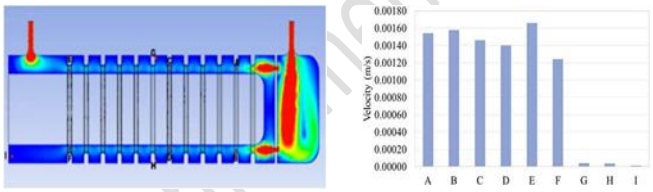


c)F22 (total fluid velocity:$8.97x10^{-3}$m/s; standard deviation:$7.34x10^{-4}$)

Figure 4. Flow simulation and fluid velocity variations of developed F20 models

Baffles have the dimensions of 5.6mm in height, 11mm in spacing and 4mm in thickness in F21 model. Aim of adding baffles was increasing velocity around the quartz holder. Total fluid velocity at given points is $8.82x10^{-3}$ m/s and standard deviation is $7.36x10^{-4}$ for F21. As can be seen from figure 4b, adding baffles greatly improved the homogeneity of flow on points A,B,C,D,E and F compared to the base model F20. Similarly, there are dead-zones created by the baffles at points G and H. These two points effect the standard deviation in a negative way, but standard deviation shows a great improvement on the straight flow line of A,B,C,D,E and F. F22 is the nozzle added version of F21. There are 6 nozzles added with a diameter of 2.5mm. The reason of adding nozzleswas to improve the flow homogeneity and velocity. Total fluid velocity at given points is $8.97x10^{-3}$ m/s and standard deviation is $7.34x10^{-4}$ for F22. As can be seen from figure 4c, nozzles slightly improved both flow homogeneity and total velocity. The points G and H are still dead-zones, which disturbs the standarddeviation data. Comparing each models developed from F20, F22 has the most even flow on a straight line outside the quartz holder.

### 3.3 Comparisons of All Models

Figure 5 and 6 show the total fluid flow velocity and standard deviation belong to all models investigated in this research. In certain cases, G, H, and I points can cause a substantial increase in the standard deviation due to the significant velocity difference between the dead zones and other points. Consequently, high standard deviation values can lead to misleading interpretations. Therefore, standard deviation 2 values, which demonstrate the standard deviation of the velocities except these points (G, H and I), were calculated and shown in Figure 7 for all models.

It can be seen from Figure 5 that F11, F14, F21 and F22 models has the highest total fluid velocity (Figure 5). This clearly shows the effect of adding baffles and nozzles. On the other hand, while still having baffles, F12 and F13 were unsuccessful in making the needed velocity difference compared to base model F10. It can be concluded that higher baffle height with lower spacing increase the total fluid velocity. These results are fully consistent with the CFD simulation study of photobioreactor with inline baffles [16]. Similarly, in another CFD study [17], the maximum turbulent kinetic energy was determined in the reactor with the widest baffle width (h=2D/3). Reducing baffle heightand spacing helped reducing dead-zones in points G and H. Compared to the standard deviation of velocity values on all points for all models, F11, F14, F21 and F22 models have the highest standard deviations due to the dead zones. However, standard deviation 2 values (Figure 7) of these pointsare lower compared to the other models. F14 has the lowest standard deviation 2 data followed by F22, F11 and F21. Similarly, in the study of CFD simulation of electrochemical filter-press reactor, adding nozzles improved the uniform distribution of the fluid flow [18].

By comparing the models with only baffles, F11 and F21, the models with baffles and nozzles, F14 and F22, we can see that adding nozzles just slightly improved the flow homogeneity and total velocity while having non-significant effect on decreasing dead-zones (G,H,I). Adding nozzles does not bring significant improvements to theexisting models, however, they require extra cost and difficulty to implement into the photoreactor. Consequently, it can be concluded that among the developed models, F11 and F21 are the most optimal models with high total velocity and homogenous flow distribution.

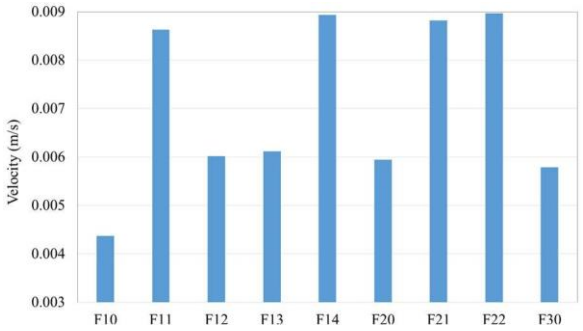

Figure 5. Total fluid flow velocity of all models

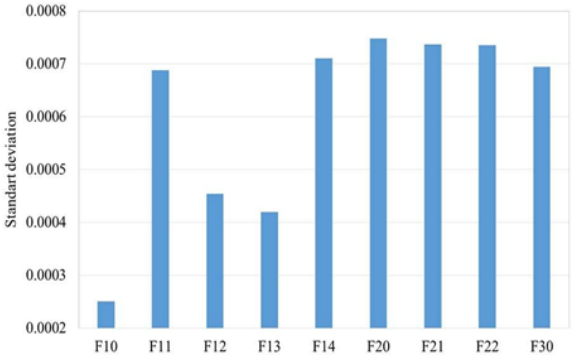

Figure 6. Standard deviation of flow velocities at all points

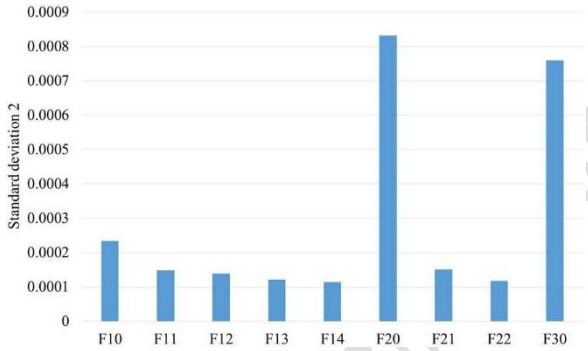

Figure 7. Standard deviation 2 of flow velocities at certain points (A,B,C,D,E,F)

## 4 Conclusion

The use of Ansys Fluent CFD software in the development of a photoreactor was investigated. Accordingly, three base models (F10, F20 and F30) were proposed first, then F10 and F20 were further developed by adding baffles and nozzles in order to increase the fluid velocity and homogeneity. The effects of baffle height and spacing on the total velocity and flow homogeneity were also investigated. All models were analyzed with total fluid velocity on selected the points and standard deviation between the velocity data. Adding baffles and nozzles increased both flow velocity and homogeneity. Increasing baffle height increased the velocity but created dead-zones, decreasing baffle height decreased both velocity and dead-zones. Adding nozzles slightly improved the total fluid velocity and homogeneity. Consequently, optimal photoreactor designs (F11 and F21), which has the highest fluid velocity and homogenous flow distribution, were determined.

This study demonstrated the significance of employing CFD software to gather crucial flow data and optimize the design of the reactor. CFD simulations not only provide researchers a detailed understanding of fluid flow patterns, temperature distribution and concentration profiles within the reactor but also it is significantly save the economy and time, which is also quite useful for industry.

## 5 Author contribution statements

Author 1 performed the simulation studies, analyzed the data and contributed to the literature review, and writing the manuscript. Author 2 designed the photoreactor, put forth the idea, evaluated the results, contributed to the literature review,and writing and reviewing the manuscript.

## 6 Ethics committee approval and conflict of interest statement

The authors declare that they have no known competing financial interests or personal relationships that could have appeared to influence the work reported in this paper, and the materials and methods used in this study do not require ethical committee permission and/or legal-special permission.

## 7 References

[1] Morris PD, Narracott A, von Tengg-Kobligk H, Soto DAS, Hsiao S, Lungu A, Gunn JP. "Computational fluid dynamics modelling in cardiovascular medicine". *Heart,* 102(1), 18- 28, 2016.

[2] Sacks MS, Yoganathan AP. "Heart valve function: a biomechanical perspective". *Philosophical Transactions of the Royal Society B: Biological Sciences,* 362(1484), 2481- 2481, 2007.

[3] Erdem M., Gok K., Gokce B., Gok A. "Numerical Analysis Of Temperature, Screwing Moment And Thrust Force Using Finite Element Method in Bone Screwing Process". *Journal of Mechanics in Medicine and Biology*, 17 (01), 1750016, 2017.

[4] Erdem M., Inal S., Taspinar F., Gulbandilar E., Gok K. "Fatigue behaviors of different materials for schanz screws in femoral fracture model using finite element analysis". *Optoelectron. Advanced Materials, Rapid Communuction*, 8(4), 576-580, 2014.

[5] Meakin P, Tartakovsky AM. "Modeling and simulation of pore-scale multiphase fluid flow and reactive transport in fractured and porous media". *Reviews of Geophysics*, 47(3), 2009.

[6] Zhao Y, Jiang M, Liu Y, Zheng J. "Particle-scale simulation ofthe flow and heat transfer behaviors in fluidized bed with immersed tube". *AIChE Journal*, 55(12), 3109-3124, 2009.

[7] Schmitt P, Windt C, Davidson J, Ringwood JV, Whittaker T. "The efficient application of an impulse source wavemaker to CFD simulations". *Journal of Marine Science and Engineering*, 7(3), 71, 2019.

[8] Córdova LJ, Rojas O, Otero B, Castillo J. "Compact finite difference modeling of 2-D acoustic wave propagation". *Journal of Computational and Applied Mathematics*, 295, 83-91, 2016.

[9] Wang K, Rallu A, Gerbeau JF, Farhat C. "Algorithms for interface treatment and load computation in embedded boundary methods for fluid and fluid–structure interaction problems". *International Journal for NumericalMethods in Fluids*, 67(9), 1175-1206, 2011.

[10] Erdem M., Fırat M., Varol Y. "Numerically investigation of MHD liquid lithium flow under cooling conditions in a circular channel". *Pamukkale University Journal of Engineering Sciences,* 24(1), 30-35, 2018.

[11] Gok K. "Investigation of the use of silicone pads to reduce the effects on the human face of classical face masks used to prevent from COVID-19 and other infections." *Proceedings of the Institution of Mechanical Engineers, Part E: Journal of Process Mechanical Engineering*, 235(5), 1742-1747, 2021.

[12] Kovacic Z, Likozar B, Hus M. "Photocatalytic $CO_2$ reduction:A review of Ab initio mechanism, kinetics, and multiscale modeling simulations". *ACS Catalysis*, 10(24), 14984-15007, 2020.

[13] Chu F, Li S, Chen H, Yang L, Ola O, Maroto-Valer M, Du X, Yang Y. "Modeling Photocatalytic Conversion of CarbonDioxide in Bubbling Twin Reactor". *Energy Conversation and Management,* 149, 514–52, 2017.

[14] Mazierski P, Bajorowicz B, Grabowska E, Zaleska-Medynska A. *Photoreactor Design Aspects and Modeling of Light.* Editors: Colmenares JC, Xu YJ. Heterogeneous Photocatalysis. 211-248, Springer-Verlag Berlin Heidelberg, Springer, 2016.

[15] Visan A, van Ommen JR, Kreutzer MT, Lammertink RGH. "Photocatalytic reactor design: Guidelines for kinetic investigation." *ACS Catalysis*, 12(13), 8066-8081, 2022.

[16] Wang L, Wang QI, Zhao R, Tao YI, Ying KZ, Mao XZ. "Novel flat-plate photobioreactor with inclined baffles and internal structure optimization to improve light regime performance". *ACS Sustainable Chemical Engineering*, 9(4), 1550–1558, 2021.

[17] Wójtowicz R, Talaga J, "Identification of Turbulent Liquid Flow in a Tubular Reactor with Different Width Baffles". *Chemical Engineering Communications,* 203(2), 161-173, 2016.

[18] Frías-Ferrer A, Tudela I, Louisnard O, Sáez V, Esclapez MD, Díez-García MI, Bonete P, González-García J. "Optimized design of an electrochemical filter-press reactor using CFD methods Author links open overlay panel". *Chemical Engineering Journal*, 169(1-3), 270-281, 2011.